Inorganic Chemistry

Article

pubs.acs.org/IC

Phosphine-Iminopyridines as Platforms for Catalytic Hydrofunctionalization of Alkenes

Ryan Gilbert-Wilson,‡ Wan-Yi Chu,‡ and Thomas B. Rauchfuss*

School of Chemical Sciences, University of Illinois at Urbana−Champaign, Urbana, Illinois 61801, United States

Supporting Information

ABSTRACT: A series of phosphine-diimine ligands were synthesized by the condensation of 2-(diphenylphosphino)aniline (PNH_2) with a variety of formyl and ketopyridines. Condensation of PNH_2 with acetyl- and benzoylpyridine yielded the $Ph_2P(C_6H_4)N{=}C(R)(C_5H_4N)$, respectively abbreviated $PN^{Me}py$ and $PN^{Ph}py$. With ferrous halides, $PN^{Ph}py$ gave the complexes $FeX_2(PN^{Ph}py)$ (X = Cl, Br). Condensation of pyridine carboxaldehyde and its 6-methyl derivatives with PNH_2 was achieved using a ferrous template, affording low-spin complexes $[Fe(PN^{H}py^{R})_2]^{2+}$ (R = H, Me). Dicarbonyls $Fe(PN^{R}py)(CO)_2$ were produced by treating $PN^{Me}py$ with $Fe(benzylideneacetone)(CO)_3$ and reduction of $FeX_2(PN^{Ph}py)$ with $NaBEt_3H$ under a CO atmosphere. Cyclic voltammetric studies show that the $[FeL_3(CO)_2]^{0/-}$ and $[FeL_3(CO)_2]^{+/0}$ couples are similar for a range of tridentate ligands, but the $PN^{Ph}py$ system uniquely sustains two one-electron reductions. Treatment of $Fe(PN^{Ph}py)X_2$ with $NaBEt_3H$ gave active catalysts for the hydroboration of 1-octene with pinacolborane. Similarly, these catalysts proved active for the addition of diphenylsilane, but not $HSiMe(OSiMe_3)_2$, to 1-octene and vinylsilanes. Evidence is presented that catalysis occurs via iron hydride complexes of intact $PN^{Ph}py$.

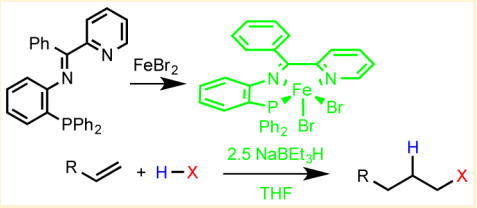

INTRODUCTION

A wide variety of coplanar, tridentate ligands have been developed for potential applications in homogeneous catalysis. Tridentate ligands with imino functionalities offer the advantage that the imine has high affinity for diverse oxidation states, and these ligands can often be prepared in a modular way, which allows for the optimization of catalyst properties.[1,2] In one of the more striking discoveries in this area, the iron diiminopyridine complexes are high-activity catalysts for hydrosilylation and hydroboration of unactivated alkenes.[3] Possibly relevant to their catalytic properties, diiminopyridines are redox-noninnocent.[4]

Within the realm of tridentate ligands, those with PNN donors are attractive alternatives to the NNN platforms. Indeed following the successes with the diiminopyridine platform, related catalysts based on Fe- and Co-derived PNN systems have been reported. Iron complexes of phosphonite-based PNN ligands exhibit high activity for hydrosilylation of unactivated alkenes even in the presence of carbonyl functional groups.[2,5] In a related study, a dialkylphosphinomethyl-bipy-derived PNN platform supports highly active catalysts for hydroboration.[6]

The present paper describes new iron complexes of PNN ligands that are hybrids of the aforementioned N−N−N and P−N−N systems. We anticipated that Fe complexes of PNN ligands might be less prone to dissociation than the Fe-diiminopyridine complexes. With the intent of obtaining permutable ligands, we were attracted to phosphine-imines, since the Schiff base condensation allows easy variation of the substituents. Complexes of phosphine-diimine ligands are an active area of research (Figure 1). The first examples were generated from the condensation of phosphinoalkylamines with diketones.[7] Highly active catalysts for the hydrosilylation of carbonyls have been developed with polydentate phosphine-imine-pyridine ligands[2,8] and diphosphine-diimine ligands.[9] PNN ligands have also been shown to support catalysts for the polymerization of ethylene.[9,10]

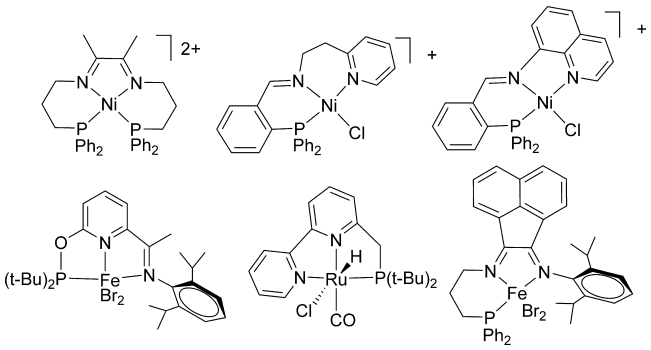

Figure 1. Complexes of representative phosphine/phosphinite-diimine ("PNN") ligands.

The new ligands reported in this work are derived from 2-(diphenylphosphino)aniline (PNH_2), which can be prepared on a large scale from triphenylphosphine and 2-chloroaniline,[11] making it a particularly accessible ligand building block.

Received: April 4, 2015
Published: May 15, 2015

DOI: 10.1021/acs.inorgchem.5b00692
Inorg. Chem. 2015, 54, 5596−5603

RESULTS

Ligand Synthesis. Phosphine-imine-pyridine ligands ($PN^{R}py^{R'}$) are in principle accessible via the condensation of (2-diphenylphosphino)aniline (PNH_2) with pyridyl ketones ($RC(O)py^{R'}$) and aldehydes ($HC(O)py^{R'}$) (Scheme 1).

Scheme 1

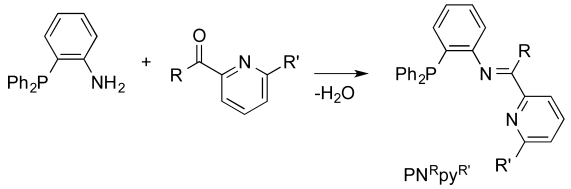

The condensation with pyridine-2-carboxaldehyde (py-2-CHO) to generate $PN^{H}py$ had been previously shown to afford phosphine oxides **A** and **B** (Scheme 2). This reaction implicates

Scheme 2. Products from the Condensation of PNH_2 and 2-Acylpyridines

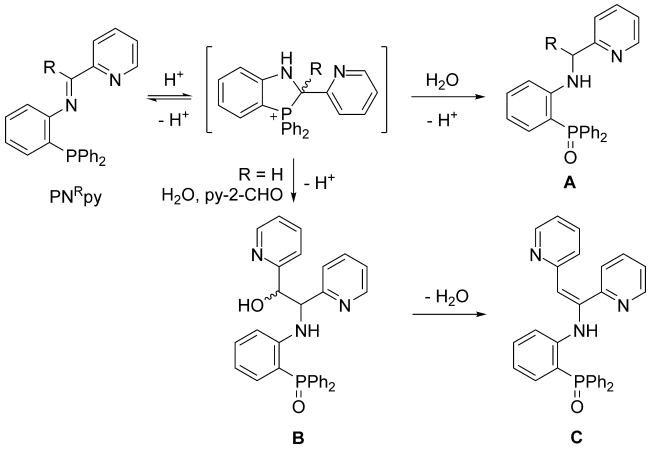

an azaphospholium intermediate, which exists in equilibrium with $PN^{H}py$.[12] Such species arise because of the adjacency of the phosphine and iminium groups, which are respectively nucleophilic and electrophilic. The phospholium intermediate is susceptible to irreversible hydrolysis by the water generated in their formation to form **A**. Conducting the condensation of PNH_2 and py-2-CHO in the presence of molecular sieves did not suppress this hydrolysis, generating **C** (see Scheme 2; for crystallographic characterization see the SI) in addition to the previously observed products.

In view of the instability of $PN^{H}py$, the condensation of pyridyl ketones with PNH_2 was examined under the assumption that the decreased electrophilicity of the ketimine would inhibit formation of the azaphospholium cation. 2-Benzoylpyridine indeed condensed with PNH_2 to give the targeted phosphine iminopyridine $PN^{Ph}py$, obtained as yellow crystals. NMR analysis indicates $PN^{Ph}py$ exists as two isomers in approximately 1:1 ratio in $CDCl_3$ solution, corresponding to the *E* and *Z* forms of the imine. Spectra were assigned to the individual isomers using $^{1}H-^{1}H$ COSY NMR spectroscopy.

Reaction of PNH_2 with 2-acetylpyridine (pyAc) afforded the phosphine oxide as the major product, but careful control of acid during the synthesis allowed isolation of small amounts of the targeted $PN^{Me}py$ ($\delta(^{31}P)$ −13.9). Hydrolysis of $PN^{Me}py$ gave the phosphine oxide, which was identified by its ^{31}P (δ 36.7) and ^{1}H NMR spectra (δ 4.59 C*H*, coupled to $-CH_3$, 6.8 Hz). The structure of this amine-phosphine oxide was confirmed by X-ray crystallography (Figure 2).

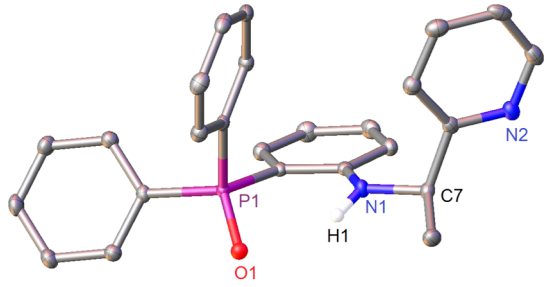

Figure 2. Representation of the solid-state structure (50% probability ellipsoids) of the phosphine oxide derived from hydration of $PN^{Me}py$. Selected hydrogen atoms are removed for clarity.

Template Syntheses of $PN^{H}py^{R'}$ Ligands. The Fe(II)-templated synthesis of tridentate phosphine-imine ligands[13] has been used to install $PN^{H}py$ on Ni(II).[12] The 2:1 ferrous complex of the same ligand was achieved analogously (Scheme 3).

Combining ferrous bromide and PNH_2 in THF solution, followed by the slow addition of py-2-CHO, quickly led to the precipitation of a blue solid. The blue solid exhibited low solubility in THF and dichloromethane, but good solubility in both MeOH and water. ESI-MS of these solutions indicated the dication $[Fe(PN^{H}py)_2]^{2+}$ (m/z = 308). The anion coformed during this condensation is likely $[FeBr_4]^{2-}$ or $[Fe_2Br_6]^{2-}$ or a mixture of the two. The $PN^{H}py$ complex was purified by conversion to $[Fe(PN^{H}py)_2](BPh_4)_2$, which was isolated as a blue solid. Although diffraction-quality crystals of $[Fe(PN^{H}py)_2]^{2+}$ could not be grown, the analogous compound $[Fe(PN^{H}py^{Me})_2](BPh_4)_2$ was prepared similarly from 6-methylpyridine-2-carboxaldehyde and identified crystallographically (Figure 3).

Crystallographic analysis of $[Fe(PN^{H}py^{Me})_2](BPh_4)_2$ confirmed the presence of an octahedral Fe center with two tridentate P−N−N ligands. The Fe−N bonds in low-spin complexes have bond lengths of ∼2.0 Å, which are noticeably shorter than observed for those in similar high-spin Fe(II) structures, which are ∼0.17 Å longer.[14] Fe−N bonds of 1.9418(12) and 2.0456(13) Å for N1 and N2, respectively, are therefore consistent with a low-spin Fe(II) center, which matches the observed ^{1}H and ^{31}P NMR data. The $PN^{H}py^{Me}$ ligands are almost planar, with an angle of 3.7° between the P1−Fe−N1 and N1−Fe−N2 planes, this small distortion indicating minimal steric interaction between the two chelating ligands.

The template synthesis was applied to ligands derived from pyAc, starting from its adduct $FeBr_2(pyAc)_2$, an octahedral, high-spin complex.[15] Treating a MeOH solution of $FeBr_2(pyAc)_2$ with 2 equiv of PNH_2 followed by ion-exchange with $NaBPh_4$ gave $[Fe(PN^{Me}py)_2](BPh_4)_2$. The BPh_4^- salts of $[Fe(PN^{R}py^{R'})_2]^{2+}$ are diamagnetic, as indicated by their simple ^{31}P and ^{1}H NMR spectra.

Complexes of the Type $FeX_2(PNN)$. Attempted synthesis of the 1:1 complex $FeCl_2(PN^{Me}py)$ generated a soluble blue intermediate prior to precipitation of the salt of $[Fe(PN^{Me}py)_2]^{2+}$. Even after filtration to remove this salt, the

DOI: 10.1021/acs.inorgchem.5b00692
Inorg. Chem. 2015, 54, 5596−5603

Scheme 3. Ligands and Complexes Reported in this Paper

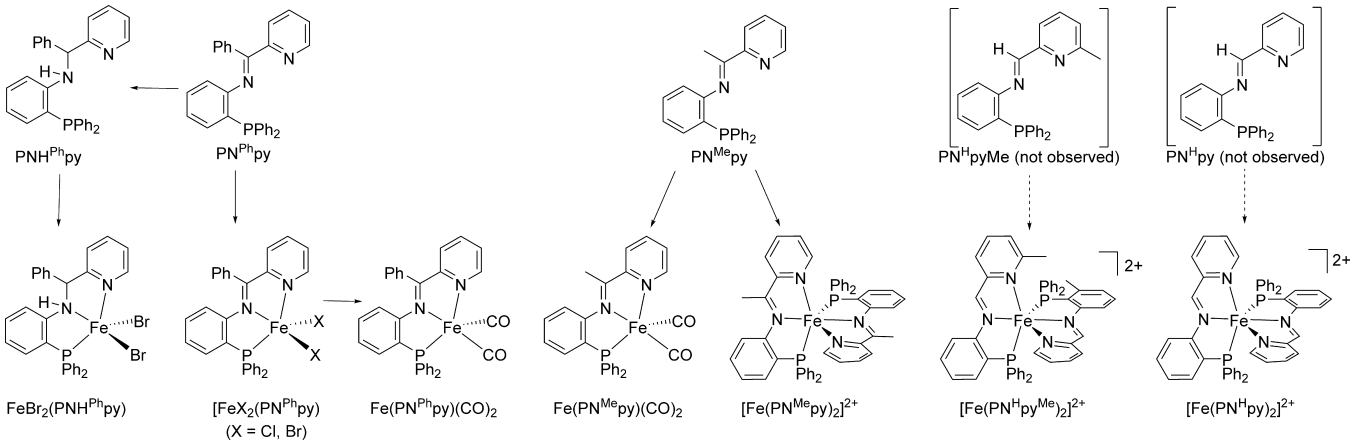

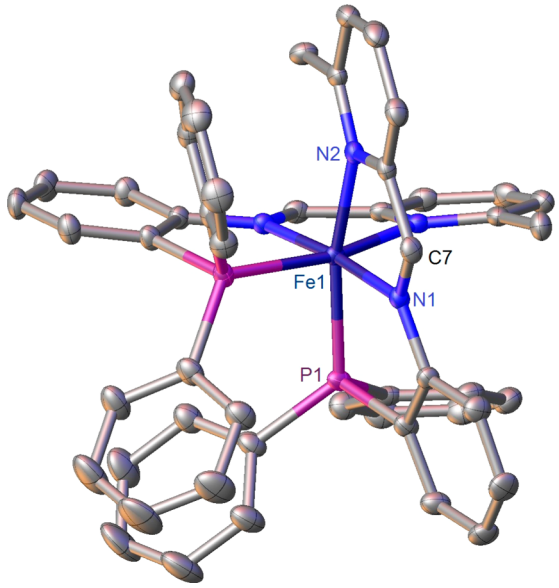

Figure 3. Representation of the solid-state structure (50% probability ellipsoids) of $[Fe(PN^{H}N^{Me})_2](BPh_4)_2$. Tetraphenylborate anions and selected hydrogen atoms have been omitted for clarity. Selected distances (Å) and angles (deg): Fe(1)−P(1), 2.2499(5); Fe(1)−N(1), 1.9418(12); Fe(1)−N(2), 2.0456(13); N(1)−Fe(1)−P(1), 85.04(4); N(1)−Fe(1)−N(2), 81.04(5).

precipitation continues, consistent with a redistribution reaction, as shown in eq 1.

$$3FeCl_2(PN^{Me}py) \rightarrow [Fe(PN^{Me}py)_2]Fe_2Cl_6 + PN^{Me}py \quad (1)$$

The problem with formation of $[Fe(tridentate)_2]^{2+}$ by ligand redistribution reactions of FeX_2(tridentate) has been noted by other workers.[16] The ligand $PN^{Ph}py$ did however afford 1:1 complexes $FeCl_2(PN^{Ph}py)$ and $FeBr_2(PN^{Ph}py)$ in good yield. Thus, THF solutions of $PN^{Ph}py$ and $FeCl_2$ or $FeBr_2$ react to give blue and green precipitates, respectively. Slow evaporation of a CH_2Cl_2 solution of $FeCl_2(PN^{Ph}py)$ afforded single crystals, which were characterized by X-ray diffraction (Figure 4). Despite its isolability, the 1:1 complex degraded at room temperature over the course of days in CH_2Cl_2 solution to $[Fe(PN^{Ph}py)_2][Fe_2X_6]$ (X = Cl, Br). The formulas of the cations were indicated by positive ion ESI mass spectrometry (m/z for dication = 425). The nature of this dianion was

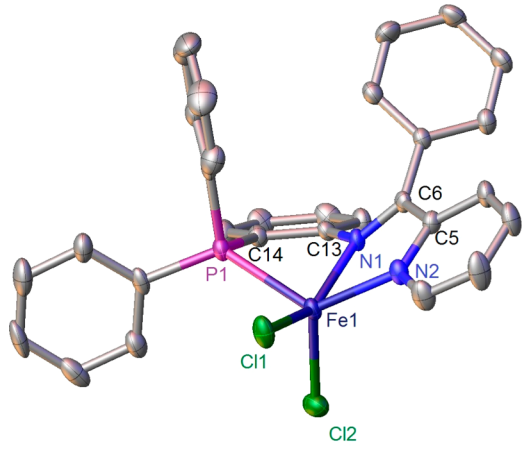

Figure 4. Representation of the solid-state structure (50% probability ellipsoids) of $FeCl_2(PN^{Ph}py)$. Selected hydrogen atoms have been omitted for clarity. Selected distances (Å) and angles (deg): Fe(1)−Cl(1), 2.2631(10); Fe(1)−Cl(2), 2.3455(10); Fe(1)−P(1), 2.4884(10); Fe(1)−N(1), 2.128(3); Fe(1)−N(2), 2.214(3); C(6)−N(1), 1.296(4); Cl(1)−Fe(1)−Cl(2), 106.21(4); N(1)−Fe(1)−P(1), 129.73(8); N(1)−Fe(1)−N(2), 73.18(10); N(2)−Fe(1)−P(1), 72.86(7).

indicated by low-resolution single-crystal X-ray diffraction (see the SI).

X-ray crystallography showed that $FeCl_2(PN^{Ph}py)$ adopts a distorted square-based pyramidal geometry (τ = 0.36, where τ is a geometrical parameter indicative of five-coordinate complex geometry where τ = 0 is perfect square pyramidal geometry and τ = 1 is perfect trigonal bipyramidal geometry).[17] A significant distortion of the $PN^{Ph}py$ ligand from planarity was observed, in contrast to the structures of the $[Fe(PN^{R}py)_2]^{2+}$ complexes described above. Since the pyridine-imine moiety remains planar, the distortion arises from rotation about the N1−C13 bond. The imine bond length is 1.296(4) Å, which is comparable to the 1.285(2) observed for the imine bond in the zinc complex $ZnCl_2(PN^{Ph}py)$, which precipitates from the combination of $ZnCl_2$ and $PN^{Ph}py$ in THF solutions (see the SI).

NMR spectroscopy studies were carried out on $FeBr_2(PN^{Ph}py)$ due to its favorable solubility. For CD_2Cl_2 solutions, the ^{1}H NMR spectrum exhibits signals over a wide chemical shift range (δ 177 to −3.70). A total of 13 of the 14 predicted signals were identified in the ^{1}H NMR spectrum of

DOI: 10.1021/acs.inorgchem.5b00692
Inorg. Chem. 2015, 54, 5596−5603

$FeBr_2(PN^{Ph}py)$. No ^{31}P NMR signal was observed. Its magnetic moment was determined as 5.1 μ_B by Evan's method.[18] These measurements are consistent with a high-spin Fe(II) (S = 2) complex, as is typical for related species.[19]

CO Derivatives. The iron dicarbonyl derivatives of the PNN ligands were prepared to facilitate analysis of the electronic properties of the $[Fe(PN^{R}py^{R'})]$ fragment. Typical for high-spin ferrous complexes,[20] the dihalides $FeX_2(PN^{Ph}py)$ do not react with CO. Addition of 2 equiv of $NaBEt_3H$ to $FeBr_2(PN^{Ph}py)$ in the presence of CO gave the dark green dicarbonyl $Fe(PN^{Ph}py)(CO)_2$ in good yield (Scheme 4). An

Scheme 4. Syntheses of $Fe(PN^{R}py)(CO)_2$

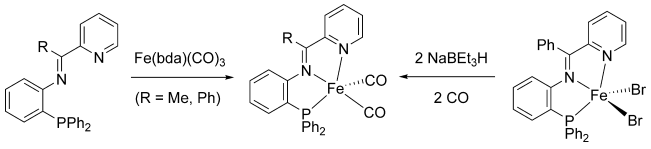

alternative method by reaction of $PN^{R}py^{R'}$ with $Fe(bda)(CO)_3$ (bda = benzylideneacetone) in THF solutions gave mixtures of phosphine-containing products (see Experimental Section). Repeated recrystallization from layering pentane on concentrated Et_2O solutions can also afford pure $Fe(PN^{Ph}py)(CO)_2$ and $Fe(PN^{Me}py)(CO)_2$ in low yield.

Crystallographic analysis confirmed the structures of the $Fe(PN^{R}py)(CO)_2$ complexes to be highly distorted square pyramidal (τ = 0.41 for $Fe(PN^{Me}py)(CO)_2$ and τ = 0.40 for $Fe(PN^{Ph}py)(CO)_2$ (Figure 5). The imine C═N bond distance in $Fe(PN^{Ph}py)(CO)_2$ (1.341(2) Å) is significantly elongated compared to that in the dihalide $FeCl_2(PN^{Ph}py)$ (1.296(4) Å), suggesting charge transfer from the iron center to the imine.[21]

The dicarbonyl complexes exhibit two strong ν_{CO} bands, which are listed in Table 1 together with data on related dicarbonyl complexes. On the basis of averaged ν_{CO} energies, $PN^{R}py$ ligands are stronger electron donors than diminopyridines and comparable to Huang's $P^{O}NN$ and Milstein's P-bipy ligands (Scheme 5).

Table 1. Cyclic Voltammetry and IR Data for Ligands and Iron Dicarbonyl Complexes vs $Fc^{+/0}$

ligand or complex[a]	reduction (V)	oxidation (V)	ν_{CO} (cm^{-1})
$PN^{Ph}py$	−2.45[b]		
$P^{O}NN$	−2.74[b]		
P-bipy			
DIP	−2.62[b]		
$Fe(PN^{Me}py)(CO)_2$	−2.37	−0.77	1943, 1884
$Fe(PN^{Ph}py)(CO)_2$	−2.25	−0.64	1961, 1907
$Fe(P^{O}NN)(CO)_2$[2]	−2.54[b]	−0.65	1956, 1902
$Fe(P\text{-bipy})(CO)_2$[23]	−2.37[b]	−0.61	1925, 1863 (CH_2Cl_2)
$Fe(DIP)(CO)_2$[24]	−2.46	−0.49	1974, 1914

[a]Ligand abbreviations: see Scheme 5. [b]Irreversible.

Scheme 5. Dicarbonyliron(0) Complexes of Pyridine-Derived Tridentate Ligands

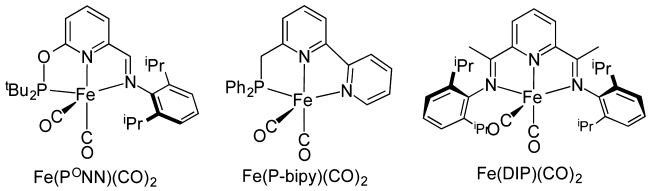

Electrochemical Measurements. The redox properties of both iron dicarbonyl complexes were examined by cyclic voltammetry (Table 1). Three redox events were observed between −0.3 and −2.8 V, one oxidation and two reductions. The reversible 1e oxidation is consistent with the behavior of other iron(0) complexes. Oxidation of $Fe(PN^{Ph}py)(CO)_2$ by $FcBF_4$ resulted in shifts of ν_{CO} from 1949 and 1890 cm^{-1} to 2005 and 1951 cm^{-1}, corresponding to $\Delta\nu_{CO} \approx 53$ cm^{-1}. The $[Fe(DIP)(CO)_2]^{+/0}$ couple is associated with $\Delta\nu_{CO} \approx 60$ cm^{-1}.[22]

The one-electron reduction of $Fe(PN^{R}py)(CO)_2$ is reversible, as for $Fe(DIP)(CO)_2$, but contrasting with the irreversibility of the couples $[Fe(P^{O}NN)(CO)_2]^{0/-}$ and $[Fe(P\text{-bipy})(CO)_2]^{0/-}$ (Figure 6). The most cathodic event

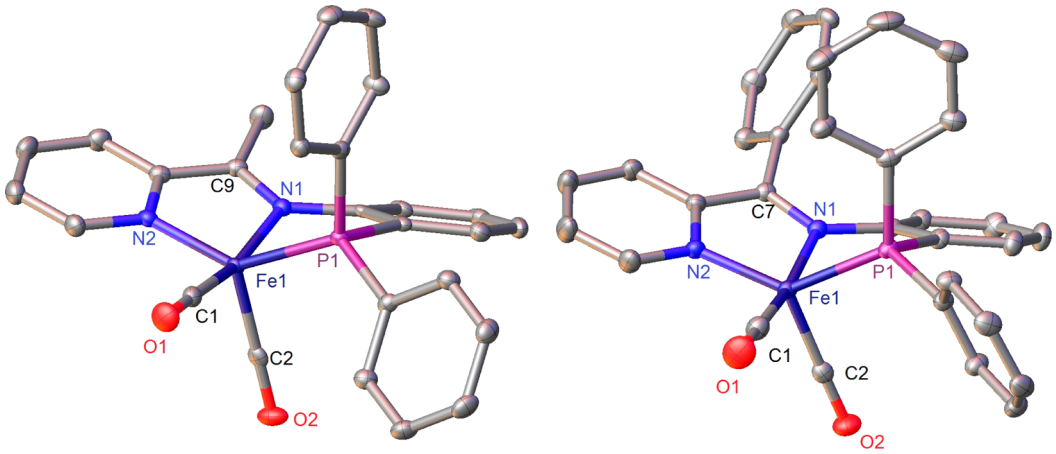

Figure 5. Representation of the solid-state structure (50% probability ellipsoids) of $Fe(PN^{Me}py)(CO)_2$ (left) and $Fe(PN^{Ph}py)(CO)_2$ (right). Solvent and hydrogen atoms have been omitted for clarity. Selected distances (Å) and angles (deg) for $Fe(PN^{Me}py)(CO)_2$: Fe(1)−P(1), 2.1759(5); Fe(1)−N(1), 1.9417(15); Fe(1)−N(2), 1.9137(16); Fe(1)−C(1), 1.7687(19); Fe(1)−C(2), 1.7638(19); O(1)−C(1), 1.157(2); O(2)−C(2), 1.156(2); C(9)−N(1), 1.339(2); N(2)−Fe(1)−P(1) 140.69(5); C(1)−Fe(1)−N(1) 116.74(7). Selected distances (Å) and angles (deg) for $Fe(PN^{Ph}py)(CO)_2$: Fe(1)−P(1), 2.1759(5); Fe(1)−N(1), 1.9137(16); Fe(1)−N(2), 1.9417(15); Fe(1)−C(1), 1.7687(19); Fe(1)−C(2), 1.7638(19); O(1)−C(1), 1.157(2); O(2)−C(2), 1.156(2); N(1)−C(7), 1.341(2); N(1)−Fe(1)−P(1) 140.69(5); N(2)−Fe(1)−C(1), 166.21(9).

DOI: 10.1021/acs.inorgchem.5b00692
Inorg. Chem. 2015, 54, 5596−5603

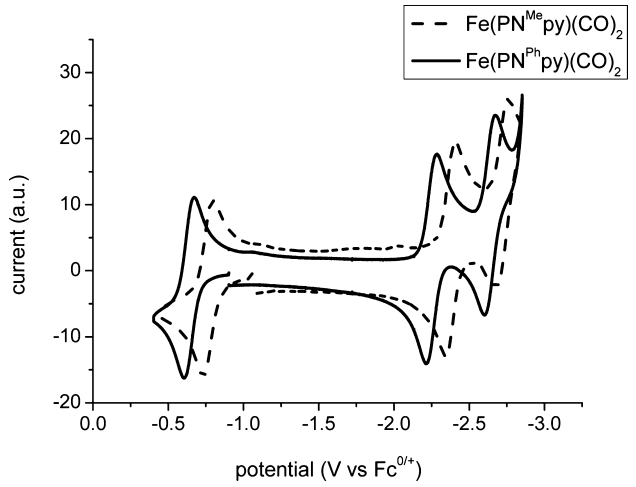

Figure 6. Cyclic voltammograms of 2 mM $Fe(PN^{Me}py)(CO)_2$ and $Fe(PN^{Ph}N)(CO)_2$ vs $Fc^{0/+}$ recorded at a scan rate of 0.1 V s^{-1} in 10 mM $[^tBu_4N]B[C_6H_4\text{-}3,5\text{-}(CF_3)_2]_4\cdot THF$ at a glassy carbon working electrode.

(ca. −2.6 V) is only partially reversible, giving i_{pa}/i_{pc} = 0.59 and 0.35 for $[Fe(PN^{Ph}py)(CO)_2]^{-/2-}$ and $[Fe(PN^{Me}py)(CO)_2]^{-/2-}$, respectively, at a scan rate of 0.1 V s^{-1}.

Similarities in potentials and reversibility of the $[Fe(PN^{R}py)(CO)_2]^{0/-}$ and $[Fe(DIP)(CO)_2]^{0/-}$ suggest that they adopt similar redox states, which are shown in Scheme 6. Reduction to the dianion $[Fe(PN^{R}py)(CO)_2]^{2-}$, which is unique to this system, is proposed to be an iron(0) center complex of the $[PN^{R}py]^{2-}$ ligand.

Phosphine-Amine-Pyridine $PNH^{Ph}py$ and $FeBr_2(PNH^{Ph}py)$. In the vast majority of systems in which $LFeX_2$ complexes (L = NNN, PNN) are used as precatalysts for hydrosilylation and hydroboration the activating agent to initiate catalysis is $NaBEt_3H$.[5,25,26,33] It was therefore of concern that the imine in the backbone of the phosphine-imine-pyridine ligand could be reduced by the $NaBEt_3H$ activator. To better understand if this process was taking place and the properties of any complexes of the reduced ligand, should they be forming, the reduced ligand $PNH^{Ph}py$ was synthesized and its complexes were investigated. Reduction of $PN^{Ph}py$ by $NaBEt_3H$ followed by protonation afforded the corresponding phosphine-amine-pyridine ($PNH^{Ph}py$). The pale yellow complex $FeBr_2(PNH^{Ph}py)$ formed as a precipitate from THF when solutions of $PNH^{Ph}py$ and $FeBr_2$ are combined. The ^1H NMR spectra of $FeBr_2(PNH^{Ph}py)$ and $FeBr_2(PN^{Ph}py)$ are similar, including the broad singlet at δ 94 and sharp singlets at δ 52.9 and 46.1, attributed to the proton resonances of the pyridine substituent.

Catalytic Studies. The complex $FeBr_2(PN^{Ph}py)$ is a precursor to an active catalyst for hydrosilylation and hydroboration. Treatment of the iron dibromide with 2.5 equiv of $NaBEt_3H$ in the presence of 1-octene and hydrofunctionalization agent gave deep brown solutions. At room temperature and with catalyst loadings as low as 0.1%, good yields were obtained of the hydroboration and hydrosilylation products. With 1-octene, both the hydrosilylation and the hydroboration gave solely anti-Markovnikov products, as seen with related iron catalysts.[2,3,5,25,26] The best conversions were found for reactions prepared by diluting 1:1 with THF. Lower conversion in neat substrate mixtures is attributed to modest catalyst solubility. The hydrosilylation of 1,1,1,3,5,5,5-heptamethyltrisiloxane ($HSiMe(OSiMe_3)_2$, HMTS) and vinylpentamethyldisiloxane ($CH_2CHSiMe_2OSiMe_3$, VPDMS) is considered a useful model for the industrial curing of siloxane polymers through hydrosilylation.[27] The hydrosilylation of VPDMS with diphenylsilane gave good yields of the anti-Markovnikov product under similar conditions and catalyst loadings to those for 1-octene. No hydrosilylation was observed for the HMTS and VPDMS, even under more forcing conditions (Table 2). Some dehydrogenative silylation was however observed under these conditions, resulting in equal quantities of $EtSiMe_2OSiMe_3$ and $(Me_3SiO)_2MeSiCHCHSiMe_2OSiMe_3$, which are respectively products of hydrogenation and dehydrogenative silylation. Dehydrogenative silylation is a known, and generally undesirable, pathway for some metal-catalyzed hydrosilylations.[28]

The structure of the active catalyst for hydroboration and hydrosilylation is uncertain, as is the case for many catalysts generated by activation of metal halides with $NaBEt_3H$.[2,5,25] Solutions of $FeBr_2(PN^{Ph}py)$ are unreactive toward pinacolborane (HBpin) and toward diphenylsilane (Ph_2SiH_2). Addition of $NaBEt_3H$ to $FeBr_2(PN^{Ph}py)$ in the absence of hydrofunctionalization agents gave less active catalysts than when both substrates are present.

We investigated the susceptibility of the ligand to attack by the $NaBEt_3H$ activator. This question was stimulated by ESI-MS analysis of the air-quenched hydrosilylation reaction mixtures that showed peaks at m/z = 461 and 483, which are assigned as the H^+ and Na^+ adducts of the phosphine oxide derived from the amine $PNH^{Ph}py$. The complex of the phosphine-amine-pyridine $FeBr_2(PNH^{Ph}py)$ (see Scheme 3) was examined as a hydrosilylation precatalyst. Upon the usual activation process, $FeBr_2(PNH^{Ph}py)$ exhibited similar activity for hydrosilylation of 1-octene with Ph_2SiH_2 (Table 2). Such solutions however were also inactive for the addition of HMTS to VPDMS.

An apparent catalytic intermediate was detected by treatment of a mixture of $FeBr_2(PN^{Ph}py)$ and Ph_2SiH_2 in Et_2O with $NaBEt_3H$. The reaction produces a thermally sensitive green species that degrades over the course of 1−2 h at room temperature. After precipitation with pentane and redissolution in THF, this green species catalyzes the hydrosilylation of 1-octene by Ph_2SiH_2 with activity comparable to the $FeBr_2(PN^{Ph}py)/Ph_2SiH_2/NaBEt_3H$ mixture. Although this

Scheme 6. Proposed Redox States of $[Fe(PN^{R}py)(CO)_2]^z$ Generated Electrochemically

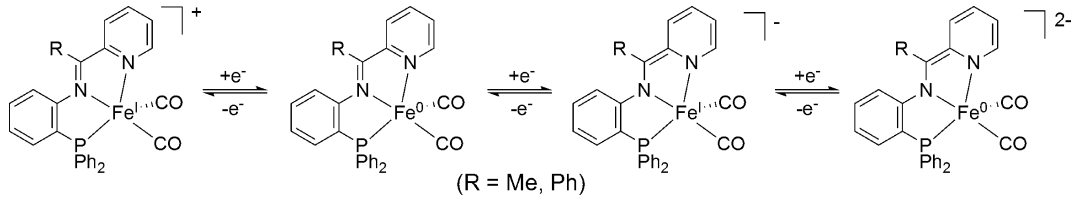

DOI: 10.1021/acs.inorgchem.5b00692
Inorg. Chem. 2015, 54, 5596−5603

Table 2. Results of Alkene Hydrofunctionalization Catalyzed by $FeBr_2(PN^{Ph}py)$ and $FeBr_2(PNH^{Ph}py)$ (23 °C, unless Otherwise Noted)

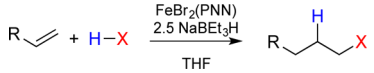

precatalyst	olefin	H-X	mol % Fe	time (h)	% yield[a]
$FeBr_2(PN^{Ph}py)$	1-octene	$H\text{-}SiHPh_2$	0.1	0.5	98
$FeBr_2(PN^{Ph}py)$	VPDMS	$H\text{-}SiHPh_2$	0.1	0.5	98
$FeBr_2(PN^{Ph}py)$	VPDMS	$H\text{-}SiMe(OSiMe_3)_2$	0.5	2.5[b]	0 (31)[c]
$FeBr_2(PN^{Ph}py)$	1-octene	H-B(pinacolate)	0.1	2	95
$FeBr_2(PNH^{Ph}py)$	1-octene	$H\text{-}SiHPh_2$	0.1	0.5	96
$FeBr_2(PNH^{Ph}py)$[a]	VPDMS	$H\text{-}SiMe(OSiMe_3)_2$	0.5	2.5[b]	0 (24)[c]

[a]Yields determined by ^1H NMR analysis vs internal standard of mesitylene. [b]55 °C (no reaction observed at 23 °C). [c]Values in parentheses are yields of the dehydrogenative silylation product.

species was not crystallized, it exhibits a simple ^{31}P NMR spectrum (δ77.2). Its ^1H NMR spectrum exhibits a doublet (10.8 Hz) at δ −14.3, arising from coupling to phosphorus. This species may be related to the σ-silane complexes of the type $Fe(diiminopyridine)(Ph_2SiH_2)_2$.[29] Quenching a solution of this green complex with CO yields $Fe(PN^{Ph}py)(CO)_2$, among other species, including free diphenylsilane. The presence of $Fe(PN^{Ph}py)(CO)_2$ indicates that the activation of imine catalysts by $NaBEt_3H$ does not involve reduction of the imine functional group.

CONCLUSIONS

This work evaluates iron complexes of a family of tridentate PNN ligands. A cautionary aspect is that certain of these pyridylimino phosphine ligands are prone to irreversible acid-catalyzed degradation, with oxidation of the phosphine. Such reactivity is a consequence of the adjacency of electrophilic iminium and nucleophilic phosphine groups and appears to proceed via the intermediacy of phosphonium salts.[30] In cases where the free ligands could not be generated from PNH_2 and pyridine carboxaldehydes, these components underwent condensation in the presence of ferrous salts, which template formation of the low-spin complexes $[Fe(PN^Hpy)_2]^{2+}$ and $[Fe(PN^Hpy^{Me})_2]^{2+}$. The drawback to this template synthesis is that the resulting, coordinatively saturated complexes are of no value for catalysis.

The ligand $PN^{Ph}py$ derived from 2-benzoylpyridine was particularly well-behaved and afforded 1:1 complexes with iron dihalides. As for related FeX_2L_3 species (L_3 = tridentate ligand),[5,25−27,29,31] the complex $FeX_2(PN^{Ph}py)$ is a precursor to a highly active catalyst for hydrosilylation and hydroboration of alkenes. An unstable catalytically active hydride intermediate was detected, and further work is aimed at characterization of related species with other ligand platforms.

Electrochemical and IR measurements on $Fe(PN^Rpy)(CO)_2$ facilitate comparisons with related ligand systems. Relative to related ligands that support hydrofunctionalization catalysis, the new phosphine-imine-pyridine ligands are stronger or comparable σ-donors. Judging from their electrochemical properties, the phosphine iminopyridines are also superior electron acceptors, undergoing not just one, but two reductions. The acceptor quality of these ligands is attributed to the 2-iminopyridine substituent.[21,32]

EXPERIMENTAL SECTION

General Considerations. Unless otherwise indicated, reactions were conducted using standard Schlenk techniques or in a glovebox under an N_2 atmosphere at room temperature with stirring. (2-Diphenylphosphino)aniline (PNH_2)[11] and $Fe(bda)(CO)_3$[33] were synthesized according to literature preparations. Toluenesulfonic acid monohydrate, pyridine-2-carboxaldehyde, 2-acetylpyridine, pinacolborane, 6-methylpyridine-2-carboxaldehyde, $FeBr_2$, $FeCl_2$, CF_3CO_2H, $NaBPh_4$, and 1 M $NaBEt_3H$ in toluene were obtained from Aldrich and used as received. ^1H (500 MHz) and ^{31}P NMR (202 MHz) spectra were acquired in Varian UNITY INOVA 500NB and UNITY 500 NB instruments, respectively. Elemental analyses were performed by the School of Chemical Sciences Microanalysis Laboratory.

$PN^{Ph}py$. 2-Benzoylpyridine (2.17 g, 11.8 mmol), PNH_2 (1.80 g, 7.90 mmol), and *p*-toluenesulfonic acid monohydrate (75 mg, 0.39 mmol) were combined in 50 mL of toluene in a Schlenk flask. The flask was fitted with a Dean−Stark trap, and the mixture was heated at reflux for 22 h. The solution was then cooled and washed with aqueous $NaHCO_3$. The organic layer was dried with $MgSO_4$, and volatiles were removed under reduced pressure. The resulting yellow oil was extracted into a small amount of CH_2Cl_2 and recrystallized by layering Et_2O and storing at −10 °C for 16 h to afford the target compound as large yellow crystals. Yield: 53% (1.87 g). ^1H NMR ($CDCl_3$) Isomer A: δ 8.57 (d, 3.6 Hz, 1H), 8.05 (d, 7.9 Hz, 1H), 7.77−7.68 (m, 1H), 7.65−7.56 (m, 1H), 7.46−6.83 (m, 17H), 7.29−7.27 (m, 1H), 6.47−6.42 (m, 1H). ^1H NMR (500 MHz, $CDCl_3$) Isomer B: δ 8.64 (d, 4.4 Hz, 1H), 7.65−7.56 (m, 1H), 7.46−6.83 (m, 17H), 7.39−7.34 (m, 1H), 7.16−7.12 (m, 1H), 6.47−6.42 (m, 1H), 6.29 (d, 7.8 Hz, 1H). ^{31}P NMR ($CDCl_3$): δ −13.6 (s, 1P, single isomer), −13.7 (s, 1P, single isomer). Anal. Calcd (found) for $C_{30}H_{23}NP\cdot H_2O$: C, 78.24 (78.25); H, 5.47 (5.39); N, 6.08 (6.09).

$[Fe(PN^Hpy^{Me})_2](BPh_4)_2$. A mixture of $FeBr_2$ (190 mg, 0.88 mmol) and PNH_2 (244 mg, 0.88 mmol) were combined in THF (6 mL) to give a yellow solution. To this solution was added 6-methylpyridine-2-carboxaldehyde (110 mg, 0.91 mmol) in THF solution (3 mL) dropwise, leading to an immediate color change to dark blue. The mixture was then stirred for 1 h, affording a blue solid precipitate that was collected and washed with THF (3 mL). This solid was then dissolved in MeOH (5 mL) followed by the slow addition of a MeOH solution (3 mL) of sodium tetraphenylborate (310 mg, 0.91 mmol), leading to the precipitation of a dark blue solid. This blue solid was collected by filtration and washed with MeOH (2 × 2 mL) and Et_2O (2 × 3 mL). Yield: 236 mg (36%). The salt $[Fe(PN^Hpy^{Me})_2](BPh_4)_2$ is insoluble in THF, sparingly soluble in CH_2Cl_2, and highly soluble in MeCN. ^1H NMR (CD_3CN): δ 9.86 (s, 2H), 8.71 (d, 8.2 Hz, 2H), 8.14 (t, 7.8 Hz, 2H), 7.84 (t, 7.5 Hz, 2H), 7.61 (m, 2H), 7.56 (t, 7.8 Hz, 2H), 7.48 (d, 7.5, 2H), 7.26 (m, 16H), 7.17 (t, 7.4 Hz, 2H), 7.14 (t, 7.4 Hz, 2H), 6.98 (m, 16H), 6.88 (t, 7.6 Hz, 4H), 6.83 (t, 7.1 Hz, 8H), 6.78 (t, 7.4 Hz, 4H), 6.52 (m, 8H), 1.74 (s, 6H); *a resonance at 5.33, assigned to CH_2Cl_2, was observed even after extended drying under vacuum. ^{31}P NMR (CD_3CN): δ 60.1 (s, 2P). Anal. Calcd (found) for $FeP_2N_4B_2C_{98}H_{82}\cdot(0.5CH_2Cl_2)$: C, 79.26 (79.00); H, 5.51 (5.59); N, 3.98 (3.74).

$[Fe(PN^{Me}py)_2](BPh_4)_2$. A solution of $FeCl_2$ (105 mg, 0.83 mmol), PNH_2 (230 mg, 0.83 mmol), and 2-acetylpyridine (110 mg, 0.91

DOI: 10.1021/acs.inorgchem.5b00692
Inorg. Chem. 2015, 54, 5596−5603

mmol) was prepared in MeOH (10 mL). The resulting deep purple mixture was stirred and heated at 50 °C for 4 h. After cooling to room temperature, the reaction solution was treated with a solution of $NaBPh_4$ in MeOH (10 mL), leading to precipitation of a blue solid. This solid was collected by filtration and washed with MeOH (2 × 2 mL) and Et_2O (2 × 3 mL) to afford $[Fe(PN^{Me}py)_2](BPh_4)_2$. Yield: 15% (93 mg). ^1H NMR (CD_2Cl_2): δ 7.83 (m, 4H), 7.73 (m, 2H), 7.70 (m, 2H), 7.41 (m, 2H), 7.35 (m, 16H), 7.21 (m, 2H), 7.16 (m, 4H), 6.98 (m, 16H), 6.90 (m, 4H), 6.87−6.80 (m, 12H), 6.63 (m, 2H), 6.56 (m, 4H), 6.32 (m, 4H), 2.64 (s, 6H), 1.55 (br, 2H); *a resonance at 5.33, assigned to CH_2Cl_2, was observed even after extended drying under vacuum. ^{31}P NMR (CD_2Cl_2): δ 60.7 (s, 2P). Anal. Calcd (found) for $FeP_2N_4B_2C_{98}H_{82}\cdot CH_2Cl_2$: C, 77.15 (77.21); H, 5.65 (5.50); N, 4.24 (4.64).

$FeBr_2(PN^{Ph}py)$. A suspension of $FeBr_2$ (80 mg, 0.37 mmol) in THF (3 mL) was treated with a THF solution of $PN^{Ph}py$ (156 mg, 0.37 mmol), causing a color change from yellow to blue-green. The mixture was stirred for 3 h, leading to a precipitation of a blue-green solid. Pentane (10 mL) was added to the suspension while stirring to further precipitate the blue-green solid. This solid was collected by filtration, washed with pentane (2 × 5 mL), and dried to give $FeBr_2(PN^{Ph}py)$ as a green powder. Yield: 89% (210 mg). ^1H NMR (CD_2Cl_2): δ 178, 75.7, 67.3, 17.8, 14.6, 13.9, 13.4, 7.71, 7.49, 5.62, 0.18, −1.66, −3.72; *a resonance at 5.33, assigned to CH_2Cl_2, was observed even after extended drying under vacuum. Anal. Calcd (found) for $C_{30}H_{23}Br_2FeN_2P\cdot 0.5(CH_2Cl_2)$: C, 52.29 (52.08); H, 3.45 (3.36); N, 4.00 (4.20).

$Fe(PN^{Ph}py)(CO)_2$. An Et_2O suspension (ca. 30 mL) containing $FeBr_2(PN^{Ph}py)$ (43 mg, 0.065 mmol) was saturated with CO. A toluene solution of $NaBEt_3H$ (1 M, 130 μL, 0.13 mmol) was diluted with Et_2O (ca. 5 mL) and transferred via cannula into the $FeBr_2(PN^{Ph}py)$ suspension under positive CO pressure. The solution gradually darkened to give a green mixture. After stirring under CO for 16 h, the solution was filtered with Celite and dried under reduced pressure. The resulting green powder was recrystallized by layering pentane over a concentrated Et_2O solution, yielding the target compound as dark green crystals. Yield: 28 mg (77%). Single crystals suitable for X-ray diffraction were also obtained this way. ^1H NMR (CD_2Cl_2): δ 9.39 (dd, 6.4, 1.4 Hz, 1H), 7.54 (ddd, 11.3, 8.2, 1.5 Hz, 4H), 7.49−7.25 (m, 12H), 7.09−7.03 (m, 2H), 7.00−6.95 (m, 1H), 6.90 (ddd, 8.5, 6.5, 1.4 Hz, 1H), 6.65−6.52 (m, 2H). ^{31}P NMR (CD_2Cl_2): δ 78.1 (s, 1P). IR (CH_2Cl_2): 1949, 1890 cm^{-1}. Anal. Calcd for $C_{32}H_{23}FeN_2O_2P\cdot 0.5Et_2O$ (found): C, 69.05 (69.1); H, 4.77 (4.90); N, 4.74 (4.94).

$PNH^{Ph}py$. To a toluene solution (3 mL) of $PN^{Ph}py$ (139 mg, 0.31 mmol) was added a 1 M toluene solution of $NaBEt_3H$ (320 μL, 0.32 mmol). The originally yellow solution gradually darkens, and bright yellow precipitates start forming after ca. 5 min. After stirring for an additional 3 h, the mixture was added to pentane (15 mL) and filtered. The bright yellow precipitate was then dissolved in MeOH (10 mL) to form a colorless solution. The solution was concentrated to ca. 2 mL and stored at −10 °C for 16 h to yield the target compound as a solid white precipitate. Yield: 98 mg (70%). ^1H NMR ($CDCl_3$): δ 8.51 (ddd, J = 4.9, 1.8, 0.9 Hz, 1H), 7.51 (td, J = 7.7, 1.8 Hz, 1H), 7.44−7.32 (m, 10H), 7.23−7.15 (m, 5H), 7.13−7.06 (m, 3H), 6.81 (ddd, J = 7.6, 6.0, 1.6 Hz, 1H), 6.60 (t, J = 7.4 Hz, 1H), 6.51−6.46 (m, 1H), 6.15 (br, 1H), 5.64−5.58 (m, 1H). ^{31}P NMR ($CDCl_3$): δ − 18.8 (s, 1P). Anal. Calcd for $C_{30}H_{25}N_2P$ (found): C, 81.06 (80.64); H, 5.67 (5.65); N, 6.30 (6.38).

$FeBr_2(PNH^{Ph}py)$. A suspension of $FeBr_2$ (48 mg, 0.22 mmol) in THF (3 mL) was treated with a THF solution of $PNH^{Ph}py$ (92 mg, 0.22 mmol). After stirring for ca. 1 min, a bright yellow solid precipitate formed. The mixture was stirred for an additional 3 h, followed by addition of pentane (10 mL). The bright yellow solid was collected by filtration, washed with pentane (2 × 5 mL), and dried to give $FeBr_2(PNH^{Ph}py)$ as a bright yellow powder. Yield: 93% (141 mg). ^1H NMR (CD_2Cl_2): δ 95.2, 52.9, 46.1, 17.3, 15.8, 13.7, 11.2, 10.2, 9.6, 8.3, 4.9, 3.8, 2.1, −1.7, −3.9, −52.27. Anal. Calcd for $C_{30}H_{25}Br_2FeN_2P\cdot 0.5H_2O$ (found): C, 53.85 (53.61); H, 3.92 (3.73); N, 4.19 (4.36).

Catalysis Experiments. A Young's NMR tube was charged with 1 mmol of olefin, 1 mmol of silane or borane, 0.001 mmol of precatalyst, 0.4 mL of d_8-THF, and two drops of the integration standard mesitylene. The ^1H NMR spectrum was recorded on the resulting slurry (colorless solution) to establish the ratio of the standard to reactants. The solution was treated with 2.5 mmol of 1 M $NaBEt_3H$ in toluene (2.5 μL). The addition gives a homogeneous brown solution (the dissolution process is noticeably exothermic for active catalysts). The tube was shaken to mix all reagents, and ^1H NMR spectra were recorded at regular intervals to monitor the rate and nature of products.

■ ASSOCIATED CONTENT

Ⓢ Supporting Information

^1H and ^{31}P NMR spectra for new compounds. X-ray crystallographic data. The Supporting Information is available free of charge on the ACS Publications website at DOI: 10.1021/acs.inorgchem.5b00692.

■ AUTHOR INFORMATION

Corresponding Author

*E-mail: rauchfuz@illinois.edu.

Author Contributions

‡R. Gilbert-Wilson and W.-Y. Chu contributed equally to this work.

Notes

The authors declare no competing financial interest.

■ ACKNOWLEDGMENTS

This research was conducted under contract DEFG02-90ER14146 with the U.S. Department of Energy by its Division of Chemical Sciences, Office of Basic Energy Sciences. We thank Drs. Danielle Gray and Jeffrey Bertke for assistance with the X-ray crystallography.

■ REFERENCES

(1) Peoples, B. C.; Rojas, R. S. In *Olefin Upgrading Catalysis by Nitrogen-Based Metal Complexes II*; Giambastiani, G., Cámpora, J., Eds.; Springer: Berlin, 2011; pp 39−75;. Gibson, V. C.; Redshaw, C.; Solan, G. A. *Chem. Rev.* **2007**, *107*, 1745−1776.

(2) Peng, D.; Zhang, Y.; Du, X.; Zhang, L.; Leng, X.; Walter, M. D.; Huang, Z. *J. Am. Chem. Soc.* **2013**, *135*, 19154−19166.

(3) Chirik, P. J. In *Catalysis without Precious Metals*; Bullock, R. M., Ed.; Wiley-VCH: Weinheim, 2010; pp 83−110.

(4) Knijnenburg, Q.; Gambarotta, S.; Budzelaar, P. H. M. *Dalton Trans.* **2006**, 5442−5448.

(5) Zhang, L.; Peng, D.; Leng, X.; Huang, Z. *Angew. Chem., Int. Ed.* **2013**, *52*, 3676−3680.

(6) Zhang, L.; Peng, D.; Leng, X.; Huang, Z. *Angew. Chem., Int. Ed.* **2013**, *52*, 3676−3680. Zhang, L.; Zuo, Z.; Leng, X.; Huang, Z. *Angew. Chem., Int. Ed.* **2014**, *53*, 2696−2700. Gunanathan, C.; Milstein, D. *Acc. Chem. Res.* **2011**, *44*, 588−602.

(7) DuBois, T. D. *Inorg. Chem.* **1972**, *11*, 718−722. DuBois, T. D.; Smith, F. T. *Inorg. Chem.* **1973**, *12*, 735−740.

(8) Ben-Daat, H.; Hall, G. B.; Groy, T. L.; Trovitch, R. J. *Eur. J. Inorg. Chem.* **2013**, *2013*, 4430−4442. Mukhopadhyay, T. K.; Flores, M.; Groy, T. L.; Trovitch, R. J. *J. Am. Chem. Soc.* **2014**, *136*, 882−885.

(9) Porter, T. M.; Hall, G. B.; Groy, T. L.; Trovitch, R. J. *Dalton Trans.* **2013**, *42*, 14689−14692.

(10) Schmiege, B. M.; Carney, M. J.; Small, B. L.; Gerlach, D. L.; Halfen, J. A. *Dalton Trans.* **2007**, 2547−2562. Small, B. L.; Rios, R.; Fernandez, E. R.; Carney, M. J. *Organometallics* **2007**, *26*, 1744−1749. Small, B. L.; Rios, R.; Fernandez, E. R.; Gerlach, D. L.; Halfen, J. A.; Carney, M. J. *Organometallics* **2010**, *29*, 6723−6731.

(11) Cooper, M. K.; Downes, J. M.; Duckworth, P. A. *Inorg. Synth.* **1989**, *29*, 129−133.

DOI: 10.1021/acs.inorgchem.5b00692
Inorg. Chem. 2015, 54, 5596−5603

(12) Doherty, S.; Knight, J. G.; Scanlan, T. H.; Elsegood, M. R. J.; Clegg, W. *J. Organomet. Chem.* **2002**, *650*, 231−248.
(13) Zuo, W.; Lough, A. J.; Li, Y. F.; Morris, R. H. *Science* **2013**, *342*, 1080−1083.
(14) Oliver, J. D.; Mullica, D. F.; Hutchinson, B. B.; Milligan, W. O. *Inorg. Chem.* **1980**, *19*, 165−169.
(15) Wei, H.-H.; Men, L.-C. *J. Inorg. Nucl. Chem.* **1978**, *40*, 221−224.
(16) Zell, T.; Langer, R.; Iron, M. A.; Konstantinovski, L.; Shimon, L. J. W.; Diskin-Posner, Y.; Leitus, G.; Balaraman, E.; Ben-David, Y.; Milstein, D. *Inorg. Chem.* **2013**, *52*, 9636−9649. Kamata, K.; Suzuki, A.; Nakai, Y.; Nakazawa, H. *Organometallics* **2012**, *31*, 3825−3828.
(17) Addison, A. W.; Rao, T. N.; Reedijk, J.; van Rijn, J.; Verschoor, G. C. *J. Chem. Soc., Dalton Trans.* **1984**, 1349−1356.
(18) Schubert, E. M. *J. Chem. Educ.* **1992**, *69*, 62.
(19) Köhler, F. H. In *eMagRes*; John Wiley & Sons, Ltd: New York, 2007. Kruck, M.; Sauer, D. C.; Enders, M.; Wadepohl, H.; Gade, L. H. *Dalton Trans.* **2011**, *40*, 10406−10415.
(20) Benito-Garagorri, D.; Lagoja, I.; Veiros, L. F.; Kirchner, K. A. *Dalton Trans.* **2011**, *40*, 4778−4792. Thammavongsy, Z.; Seda, T.; Zakharov, L. N.; Kaminsky, W.; Gilbertson, J. D. *Inorg. Chem.* **2012**, *51*, 9168−9170.
(21) Bart, S. C.; Chłopek, K.; Bill, E.; Bouwkamp, M. W.; Lobkovsky, E.; Neese, F.; Wieghardt, K.; Chirik, P. J. *J. Am. Chem. Soc.* **2006**, *128*, 13901−13912.
(22) Tondreau, A. M.; Milsmann, C.; Lobkovsky, E.; Chirik, P. J. *Inorg. Chem.* **2011**, *50*, 9888−9895.
(23) Zell, T.; Milko, P.; Fillman, K. L.; Diskin-Posner, Y.; Bendikov, T.; Iron, M. A.; Leitus, G.; Ben-David, Y.; Neidig, M. L.; Milstein, D. *Chem.—Eur. J.* **2014**, *20*, 4403−4413.
(24) Darmon, J. M.; Turner, Z. R.; Lobkovsky, E.; Chirik, P. J. *Organometallics* **2012**, *31*, 2275−2285.
(25) Zhang, L.; Zuo, Z.; Leng, X.; Huang, Z. *Angew. Chem., Int. Ed.* **2014**, *53*, 2696−2700.
(26) Obligacion, J. V.; Chirik, P. J. *Org. Lett.* **2013**, *15*, 2680−2683.
(27) Tondreau, A. M.; Atienza, C. C. H.; Weller, K. J.; Nye, S. A.; Lewis, K. M.; Delis, J. G. P.; Chirik, P. J. *Science* **2012**, *335*, 567−570.
(28) Atienza, C. C. H.; Diao, T.; Weller, K. J.; Nye, S. A.; Lewis, K. M.; Delis, J. G. P.; Boyer, J. L.; Roy, A. K.; Chirik, P. J. *J. Am. Chem. Soc.* **2014**, *136*, 12108−12118.
(29) Bart, S. C.; Lobkovsky, E.; Chirik, P. J. *J. Am. Chem. Soc.* **2004**, *126*, 13794−13807.
(30) Schnell, A.; Tebby, J. C. *J. Chem. Soc., Perkin Trans. 1* **1977**, 1883−1886. Landvatter, E. F.; Rauchfuss, T. B. *J. Chem. Soc., Chem. Commun.* **1982**, *0*, 1170−1171.
(31) Sylvester, K. T.; Chirik, P. J. *J. Am. Chem. Soc.* **2009**, *131*, 8772−8774. Darmon, J. M.; Turner, Z. R.; Lobkovsky, E.; Chirik, P. J. *Organometallics* **2012**, *31*, 2275−2285. Obligacion, J. V.; Chirik, P. J. *J. Am. Chem. Soc.* **2013**, *135*, 19107−19110. Chen, J.; Cheng, B.; Cao, M.; Lu, Z. *Angew. Chem., Int. Ed.* **2015**, *127*, 4744−4747.
(32) Kaim, W.; Schwederski, B. *Coord. Chem. Rev.* **2010**, *254*, 1580−1588.
(33) Alcock, N. W.; Richards, C. J.; Thomas, S. E. *Organometallics* **1991**, *10*, 231−238.

DOI: 10.1021/acs.inorgchem.5b00692
Inorg. Chem. 2015, 54, 5596−5603